American Academic Scientific Research Journal for Engineering, Technology, and Sciences

ISSN (Print) 2313-4410, ISSN (Online) 2313-4402

https://asrjetsjournal.org/index.php/American_Scientific_Journal/index

Urban Heat Island (Uhi) Effect: The Rise of Land Surface Temperature in Cebu City, Philippines

Menzuela Ancheta-Comora[a], Natalino de Araújo[b*], Edilyn Lopez[c], Charles Frank Caramihan[d], Garry Marapao[e]

[a]College of Agriculture, New Era University– Rizal Branch, Pinugay, Rizal

[b]Universidade Nacional Timor Lorosa'e, Timor Leste

[c,d]School of Environmental Science, University of the Philippines, Los Baños

[e]College of Agriculture, Forestry, and Environmental Sciences - Mindanao State University at Naawan, Philippines

[a]Email: menzuelahancheta@gmail.com, [b]Emaill: linonata39@gmail.com, [c]Email: Ellopez1@up.edu.ph

[d]Emaill:Clcaramihan1@up.edu.ph, [e]Email: gcmarapao@up.edu.ph

Abstract

Temperature differences between the urban and surrounding areas have resulted from rapid urbanization. This study tries to systematically understand the urban heat island phenomenon in Cebu City by determining the land surface temperature using satellite images in 2010 and 2018. Land Surface Temperature (LST) was determined using the Surface Energy Balance Algorithm for Land (SEBAL) approach. The results were correlated to spatial metrics to identify its influence on the spatial variation of LST in Cebu City. Results indicated that the mean LST in Cebu City increased from 22^0C to 25^0C from 2010 to 2018. In 2018, the built-up area contributed the most LST, followed by forest and bare land, with 28.40 0C, 26.25 0C, and 25.85 0C, respectively. The results indicated that the landscape metrics are highly negatively correlated to LST, mainly attributed to the increase in forest area in Cebu City.

Keywords: urban heat island; remote sensing; SEBAL; landscape metrics; Cebu City.

1. Introduction

Urbanization negatively impacts the environment mainly through the production of pollution, the modification of the physical and chemical properties of the atmosphere, and the covering of the soil surface.

Received: 2/25/2023
Published: 4/20/2023

----

* Corresponding author.

Considered to be a cumulative effect of all these impacts is the Urban Heat Island (UHI), defined as the rise in temperature of any man-made area, resulting in a well-defined, distinct "warm island" among the "cool sea" represented by the lower temperature of the area's nearby natural landscape [10]. Though heat islands may form in any rural or urban area, cities are favored at any spatial scale since their surfaces are prone to release massive amounts of heat [9]. Nonetheless, the UHI negatively impacts residents of urban-related environs, humans, and their associated ecosystems far away from cities. UHIs have been indirectly related to climate change due to their contribution to the greenhouse effect and global warming. UHI is classified into two types: surface UHIs, measured based on Land Surface Temperature (LST), and atmospheric UHIs, measured based on air temperature, and are often classified into canopy layer, surface, and boundary layer UHIs [5]. The Surface Energy Balance Algorithm for Land (SEBAL) is one method to measure the land surface temperature. It is a physically based analytical image processing method that evaluates the energy balance components and determines the last as the residual. SEBAL is based on the computation of energy balance parameters from multi-spectral satellite data [12]. The Canopy Layer Heat Island (CLHI) and the Boundary Layer Heat Island (BLHI) refer to the warming of the urban atmosphere, whereas the Surface Heat Island (SHI) refers to the warming of the urban space. The CLHI exists in the layer of air where people live, from the ground to below the tops of trees and roofs; BLHII starts from the rooftop and treetop level and extends up to the point where urban landscapes no longer influence the atmosphere. Several factors that affect the UHI phenomenon are human activities, vehicles, air conditioning, industrial activities, urban geometry, sky view factor, and air pollution, among others. It is well-known that urbanization's progressive replacement of natural surfaces by built surfaces constitutes the leading cause of UHI formation. More specifically, the formation of the UHI is influenced by landscape changes due to urban development in which open lands and green spaces are converted into built-up lands or impervious surfaces (e.g., buildings, roads, etc.) and by the resulting anthropogenic heat [5, 6, 14]. Natural surfaces are often composed of vegetation and moisture-trapping soils. Therefore, they utilize a relatively substantial proportion of the absorbed radiation in the evapotranspiration process and release water vapor to cool the air in their vicinity. In contrast, built surfaces comprise a high percentage of non-reflective and water-resistant construction materials. Consequently, they absorb a considerable proportion of the incident radiation released as heat. Thus, landscape compositions such as fractions of impervious surface and green space, which, in most cases, are determined from remote sensing data, have been important inputs to studying UHI formations [1, 6, 8, 15]. Additional factors such as the scattered and emitted radiation from atmospheric pollutants to the urban area, the production of waste heat from air conditioning and refrigeration systems and industrial processes and motorized vehicular traffic (i.e., anthropogenic heat), and the obstruction of rural air flows by the windward face of the built-up surfaces have been recognized as additional causes of the UHI effect. Scientists use direct and indirect methods, numerical modeling, and estimates based on empirical models to identify urban heat islands. Researchers often use remote sensing, an indirect measurement technique, to estimate surface temperatures. Today, urban-rural gradient analysis, multiresolution analysis, and spatial metrics are among the most popular approaches for quantifying the effects of urban landscape patterns.

2. Review of Related Literature

Cebu City is the capital of the island province of Cebu, located 550 km southeast of Manila in the center of the Visayan Islands region. Its 1990 population stood at 610,417, with the Cebu City metropolitan area, including

Cebu, Mandaue, and Lapu-Lapu Cities, and two adjacent municipalities, having a combined population of I.1 million. Cebu City has a land area of 292 square kilometers, with about 56 square kilometers classified as urban areas and 235 sq. meters classified as rural areas. The city's provincial capital is bounded by the following adjacent cities: Mandaue City to the northeast, Toledo City to the west, and Talisay City to the south. Cebu City is subdivided into 80 barangays grouped into two congressional districts, with 46 barangays in the northern and 34 in the southern districts.

In the recent past, urban heat island was an almost unknown phenomenon in urban planning. A preliminary study conducted in Cebu City provided initial evidence that some areas are slowly developing their urban heat climate. Despite being located in a coastal city, the cooling effect of nearby coastal waters may only exert a limited influence in moderating urban microclimate in the long run. According to the study of [13], the dense built-up of urban spaces, traffic, lack of open or green spaces, construction activities, urban morphology, and meteorological conditions related to climate change, among others, may significantly contribute more heat stress to rapidly developing urban areas in Cebu City.

UHI was quantified by measuring the differences in surface and air temperature of urban areas against the temperatures in rural areas. The overall mean temperature difference was measured in Cebu City. Elevation was found to be the best predictor of UHI in Cebu City. The results matched positively with the study of [7], who found that elevation was a major factor in determining the lowest temperature contrast between two different stations in the coastal city of Thessaloniki, Greece. Conferring to the study of [13], it is possible that as Cebu City reaches its peak of development around 10-20 years from now, the population will be a significant predictor of UHI.

3. Methodology

3.1 Study area

Cebu City is considered the first class highly urbanized city in the province of Cebu in Central Visayas, with a total population of 922,611 as of 2015. With this population, Cebu City is the most populous in the Visayas region and the fifth most populated city in the Philippines. Mandaue City and Consolacion bound Cebu City in the northeast, Toledo City and the towns of Balamban and Austrias to the west, and Talisay City and Minglanilla to the south (**Figure 1**).

According to the modified Corona Classification of Climate, Cebu City is under the Type IV classification, with more or less evenly distributed throughout the year. This climate type resembles the second type more closely since it has no dry season.

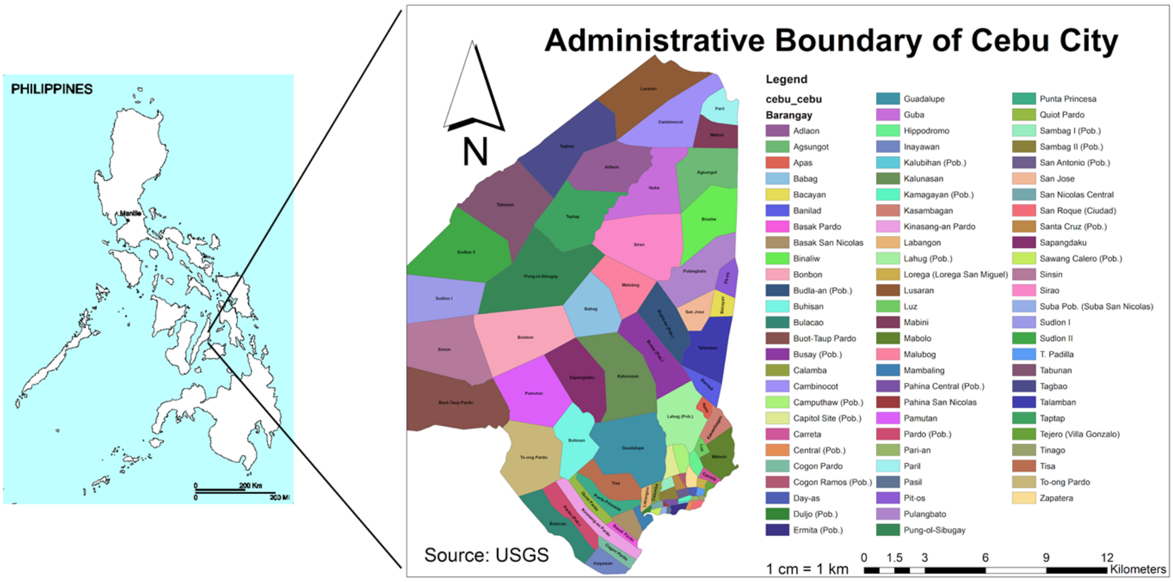

Figure 1: Location and administrative boundaries of Cebu City, Philippines.

3.2 Data Description and Processing

The data gathered were images from Landsat 5 and 8 with ten years intervals (2010 and 2018). The images were downloaded from the United States Geological Survey (USGS) Earth Explorer's website (www.earthexplorer.usgs.gov).

3.2.1 Landsat 8

The image (2018) from Landsat 8 has nine multispectral bands and two thermal bands. Bands 1-7 and 9 have 30 meters resolution while band 8 has 15 meters resolution. Lastly, bands 10 and 11 are the thermal bands that collect images at 100 meters and resample the images to 30 meters. The Landsat 8's band assignment summary is below (see **Table 1**).

Table 1: Band designation of Landsat 8.

Bands	Wavelength (micrometers)	Resolution (meters)
Band 1 - Ultra Blue (coastal/aerosol)	0.435 - 0.451	30
Band 2 - Blue	0.452 - 0.512	30
Band 3 - Green	0.533 - 0.590	30
Band 4 - Red	0.636 - 0.673	30
Band 5 - Near Infrared (NIR)	0.851 - 0.879	30
Band 6 - Shortwave Infrared (SWIR) 1	1.566 - 1.651	30
Band 7 - Shortwave Infrared (SWIR) 2	2.107 - 2.294	30
Band 8 - Panchromatic	0.503 - 0.676	15
Band 9 - Cirrus	1.363 - 1.384	30
Band 10 - Thermal Infrared (TIRS) 1	10.60 - 11.19	100 * (30)
Band 11 - Thermal Infrared (TIRS) 2	11.50 - 12.51	100 * (30)

*Resampled to 30m

Source: USGS

3.2.2 Landsat 5

The Image from Landsat 5 (2010) has six spectral bands and one thermal band. Bands 1-5 and 7 are spectral bands that have 30 meters resolution, while band 6 is a thermal band collected at 120 meters but resampled to 30 meters. Below is the summary of the band designation of Landsat 5 (**Table 2**).

Table 2: Landsat 5's band designations.

Landsat 4-5 Thematic Mapper (TM)	Bands	Wavelength (micrometers)	Resolution (meters)
	Band 1 - Blue	0.45-0.52	30
	Band 2 - Green	0.52-0.60	30
	Band 3 - Red	0.63-0.69	30
	Band 4 - Near Infrared (NIR)	0.76-0.90	30
	Band 5 - Shortwave Infrared (SWIR) 1	1.55-1.75	30
	Band 6 - Thermal	10.40-12.50	120* (30)
	Band 7 - Shortwave Infrared (SWIR) 2	2.08-2.35	30

*Resampled to 30m

Source: USGS

3.2.3 Land surface temperature retrieval

Land Surface Temperature (LST) was computed using Surface Energy Balance Algorithm for Land (SEBAL). The values used in the band math and the equation used to calculate the LST are listed below in Table 3. The workflow for generating LST from satellite images is presented in **Figure 2**.

Table 3: Summary of equations used in the calculations.

p (Brightness Temperature)	$h\left(\frac{c}{s}\right)(1.438X10^{-2}mk)$
h (Plank's constant)	$6.626X10^{-34}\,Js$
S (Boltzmann constant)	$1.38\,X\,10^{-23}\,J/K$
C (Velocity of light)	$2.998\,X\,10^{8}\,m/s$
e	0.004Pv+0.986
Pv	$\left(\frac{NDVI-NDVImin}{NDVImax-NDVImin}\right)^2$
W (Wavelength of emitted Radiance)	(11.5 micrometers)
BT (Brightness Temperature at Satellite)	*see metadata file
LST (Land Surface Temperature)	$\frac{BT}{1}$ $\frac{BT}{p}+w$ (ln e)

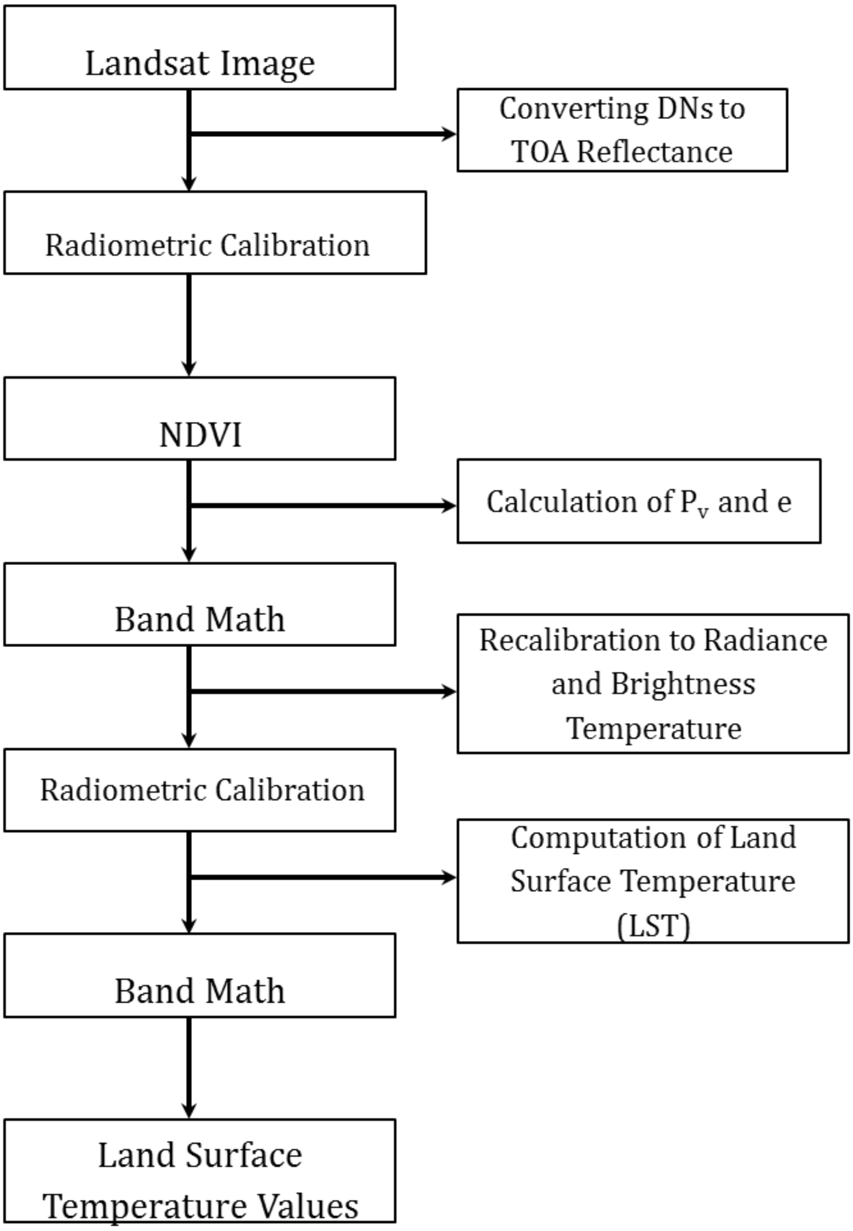

Figure 2: Workflow of LST retrieval.

3.2.4 Land cover mapping and thematic change

The obtained satellite images were then fed to ENVI software for radiometric calibration, classification workflow using the unsupervised method, and thematic change assessment.

Land cover classifications are water, forest, clouds, built-up, and bare land. Clouds were considered land cover as the satellite images weren't free of clouds.

The produced thematic maps were fed to ArcGIS for further analysis. Classification did not undergo accuracy assessment as it needed more time for ground truthing. The classified images are then for this purpose only.

3.2.5 Spatial metrics analysis

The study used the landscape ecological approach to determine spatial metrics' influence on LST's spatial variability. The clipped or subset images of the study area were further analyzed using the landscape metrics software FRAGSTATS. The study used the following metrics at the class level: mean patch size (Area_Mn), mean shape index(Shape_Mn), and aggregation index (AI). Details of the metrics used are presented in **Table 4.**

Table 4: Landscape metrics used in the study adapted from [6].

Metric (class-level)	Description
Mean patch size (AREA_MN)	• AREA_MN is a measure of patch area or size. • AREA_MN equals the sum, across all patches of the corresponding patch type, of the corresponding patch metric values, divided by the number of patches of the same type. • $AREA\_MN(ha) = \frac{1}{10{,}000 \times n} \times \sum_{i=1}^{n} x_i$
Mean shape index (SHAPE_MN)	• SHAPE is the simplest and perhaps most straightforward measure of shape complexity. • SHAPE_MN equals patch perimeter (m) divided by the square root of patch area (m^2), adjusted by a constant to adjust for a square standard and divided by the number of patches of the same type. • $SHAPE\_MN = \frac{1}{n} \times \frac{0.25\ p_i}{\sqrt{x_i}}$ • SHAPE_MN equals 1 when the patch is square and increases without limit as patch shape becomes more irregular.
Aggregation index (AI)	• AI equals the number of like adjacencies involving the corresponding class, divided by the maximum possible number of like adjacencies involving the corresponding class, which is achieved when the class is maximally clumped into a single, compact patch; multiplied by 100 (to convert to a percentage). • $AI(\%) = \left(\frac{g_i}{max - g_i}\right) \times 100$ • AI equals 0 when the focal patch type is maximally disaggregated (i.e. when there are no like adjacencies). It increases as the focal patch type is increasingly aggregated and equals 100 when the patch type is maximally aggregated into a single, compact patch.

Notations: x_i area of patch i; p_i perimeter of patch i; n number of patches; g_i number of like adjacencies (joins) between pixels of patch type (class) i based on the single-count method; $max - g_i$ maximum number of like adjacencies (joins) between pixels of patch type (class) i based on the single-count method. See McGarigal et al. (2012) for details.

3.2.6 Statistical analysis

Descriptive statistics were used to describe the results of the LST retrieval and correlation analysis using MS Excel to determine the relationship between landscape metrics and LST in the study area.

3. Results and Discussion

4.1 LST and land cover maps

The computed land surface temperature (LST) of Cebu City from the satellite images obtained from Landsat 5 and 8 for the years 2010 and 2018, respectively, is presented in Figure 3. Results showed that in 2010, LST ranged from 18^0C to 33^0C with an average of about 22^0C. On the other hand, LST for the year 2018 ranges from 18^0C to as high as 37.6^0C with an average of about 25^0C.

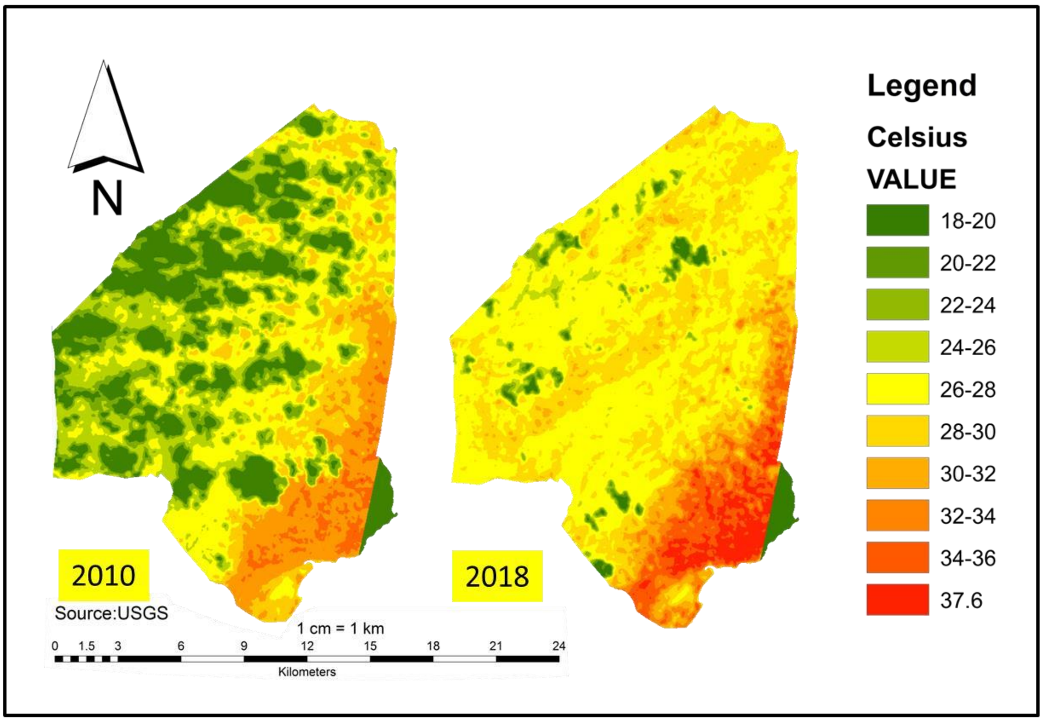

Figure 3: Land surface temperature map of Cebu City for the years 2010 and 2018.

The classified land cover map of Cebu City obtained from Landsat 5 and 8 for 2010 and 2018 is presented in **Figure 4**. The most notable change in the landscape between the two periods is the increase in built-up areas for 2018 at about 1000 hectares. The detail of other land conversions in Cebu City is presented in **Table 5**.

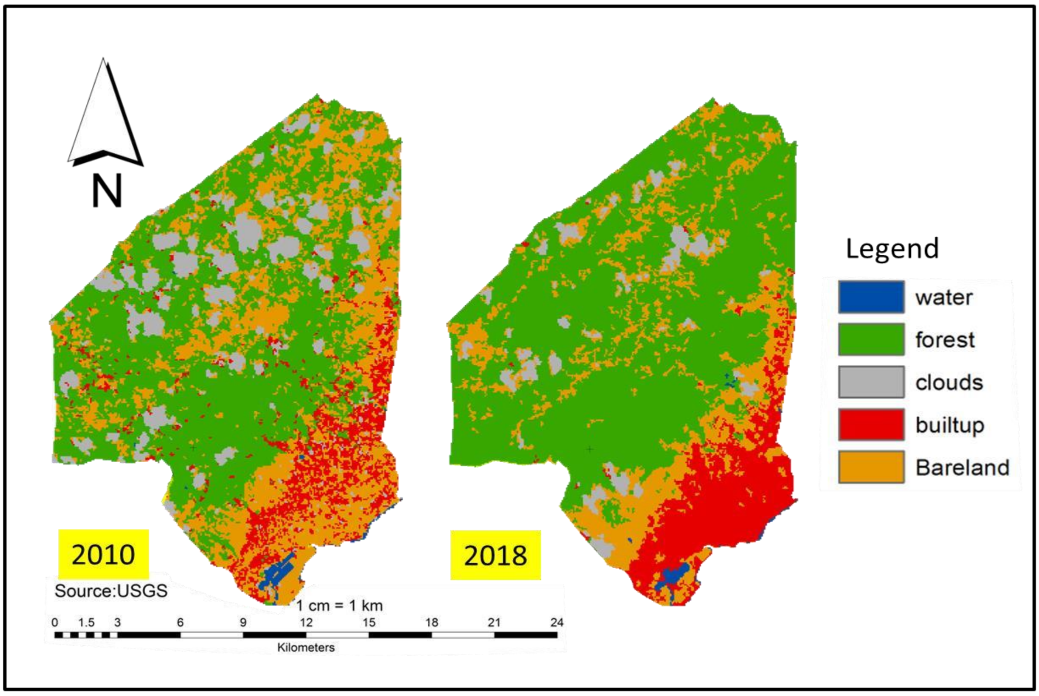

Figure 4: Land cover map of Cebu City for the years 2010 and 2018.

Table 5: Land cover thematic change in Cebu City (2010 to 2018).

		2018 (hectares)					
	Classification	**Bareland**	**Built-up**	**Clouds**	**Forest**	**Water**	**Total**
2010 (hectares)	**Bareland**	3393.99	1993.41	257.31	3913.02	9.9	9567.63
	Built-up	833.04	1801.62	42.3	218.88	6.03	2901.87
	Clouds	547.2	118.62	150.57	2736.27	1.17	3553.83
	Forest	1457.73	43.02	818.46	17053.74	4.32	19377.27
	Water	6.39	51.84		1.26	1881.81	1941.3
	Total	6238.35	4008.51	1268.64	23923.17	1903.23	37341.9

Overlaying the data from LST and land cover maps in Cebu City using GIS software showed that land surface temperature was generally higher in 2018 than in 2010. Increased LST can be attributed to increased impervious surfaces, particularly in built-up areas. Moreover, this is also evident in the LST results of the study for built-up, which is the highest among the different land cover at 28.40 ^{0}C. The increase in impervious surfaces is highly related to the heat island effect and can significantly alter the local climate. The mean temperature for the different land cover in Cebu City is presented in **Table 6**.

Table 6: The mean temperature of the different land classifications in Cebu City (2010 and 2018).

	Mean Temperature (^{0}C)	
Classification	**2010**	**2018**
Bareland	22.30	25.85
Built-up	24.26	28.40
Forest	21.25	26.25

4.2 LST and landscape metrics

The study also considered landscape metrics to assess which spatial metrics of the different land cover, particularly patches of built-up, bare land, and forest lands, are likely to influence the spatial variation of LST in Cebu City. Landscape metrics values per land cover and its corresponding LST are presented in Table 7. Based on the results for the aggregation index, the built-up area had increased from 65% to 95%, while other land cover remained almost the same from 2010 to 2018. A notable increase in mean area for built-up from 9 has to 81 hectares and forest from 98 to 390 hectares was observed between 2010 and 2018. Lastly, the mean shape for all land cover patches from 2010 to 2018 had not changed a bit and was more than 1, indicating irregular shape for all patches.

Correlation analysis was carried out for the landscape metrics and mean LST from 2010 to 2018 in Cebu City (**Table 8).** Results indicated that most landscape metrics negatively correlate to LST for both periods. Furthermore, temperature somehow decreases as the landscape metrics used in the study (area, shape, and aggregation index) increase. This finding can be attributed to the high growth in forest areas from 2010 to 2018 in Cebu City. However, looking alone into the built-up area, results indicated that LST in such land cover is higher than in another land cover.

Table 7: Landscape metrics and LST values in Cebu City.

Classification	Landscape Metrics	Values (2010)	LST (2010)	Values (2018)	LST (2018)
Built-up	AI %	65.07	24.26	91.03	28.40
Bareland	AI %	74.02	22.30	74.92	25.85
Forest	AI %	86.97	21.25	93.50	26.25
Built-up	Area-Mn	9.02	24.26	80.75	28.40
Bareland	Area-Mn	17.57	22.30	22.55	25.85
Forest	Area-Mn	97.63	21.25	390.33	26.25
Built-up	Shape_Mn	1.34	24.26	1.55	28.40
Bareland	Shape_Mn	1.45	22.30	1.71	25.85
Forest	Shape_Mn	1.45	21.25	1.59	26.25

Table 8: Correlation of landscape metrics and mean LST in Cebu City.

Year	Landscape metrics	Correlation
2010	Shape - LST	-0.94
2010	Area-LST	-0.82
2010	AI-LST	-0.96
2018	Shape - LST	-0.77
2018	Area-LST	-0.23
2018	AI-LST	0.52

The study results indicated that increased LST is mainly observed in land cover with impervious surfaces such as built-up areas. Coupled with the increase in impervious surfaces is the increase in temperature. If left unmanaged can eventually disrupt critical ecological processes, particularly diversity, food production, water cycle, nutrient cycling, energy flow, and community dynamics [2]. In addition, UHI affects human populations, particularly in urban areas where heat stress can occur. People exposed to high temperatures can experience heat stroke, exacerbating existing health conditions such as cardiovascular and cerebrovascular disease, diabetes, chronic obstructive pulmonary disease, pneumonia, asthma, and influenza [11].

4. Conclusion and Recommendation

The study assessed the Urban Heat Island (UHI) phenomenon in Cebu City by determining the land surface temperature using satellite images from 2010 and 2018. LST was determined using the Surface Energy Balance Algorithm for Land (SEBAL) approach. The results were correlated to spatial metrics to identify its influence on the spatial variation of LST in Cebu City. Results indicated that the mean LST in Cebu City increased from

22^0C to 25^0C from 2010 to 2018. The land cover that contributed the highest LST for 2018 is the built-up area, followed by forest and bare land with 28.40 ^{0}C, 26.25 ^{0}C, and 25.85^{0}C, respectively. LST results were then correlated to landscape metrics such as mean area, mean shape, and aggregation index. The results indicated that the landscape metrics are highly negatively correlated to LST, mainly attributed to the increase in forest area in Cebu City.

However, increased LST in the urban area is noteworthy as the site is observed to be increasing over time and, if neglected, can have detrimental effects on fundamental ecological processes and the human population. It is therefore recommended that mitigation measures to counter the impact of UHI are implemented as early as now. Some of the UHI mitigation measures include tree/shrub planting to increase vegetation, including green buildings, usage of highly reflective roofing and exterior materials in buildings, saving energy, particularly air conditioning equipment, which releases heat in its exhaust, and increasing open and airy space [16, 4].

5. Limitations/Constraints of the Study

The study may have data limitations, such as the availability of reliable and accurate data on land surface temperature, land use and land cover, and weather variables, which may impact the accuracy and validity of the results. The study also focuses on a particular scale of analysis, such as a specific city or region, which may limit the generalizability of the findings to other locations. Another one is the study's timeframe, which may impact the ability to detect long-term trends in the UHI effect and evaluate the effectiveness of mitigation strategies over time.

Acknowledgments

We thank our family and friends for their unending support and the University of the Philippines Los Baños. Thanks, will also be directed to Dr. Cristino Tiburan Jr. for his help in this research.

References

[1] A. Buyantuyev & J. Wu. (2010). Urban heat islands and landscape heterogeneity: linking spatiotemporal variations in surface temperatures to land-cover and socioeconomic patterns. *Landscape ecology*, *25*(1), 17-33.

[2] S. V. Chithra, M.H. Nair, A. Amarnath, & N.S. Anjana. (2015). Impacts of impervious surfaces on the environment. *International Journal of Engineering Science Invention*, *4*(5), 27-31.

[3] EPA. 2003. Beating the Heat: Mitigating Thermal Impacts. Nonpoint Source News-Notes. 72:23-26.

[4] EPA. 2017. Reduce heat island effect. Retrieved from https://www.epa.gov/green-infrastructure/reduce-urban-heat-island-effect.

[5] EPA. 2018. Heat island effect. Retrieved from https://www.epa.gov/heat-islands

[6] R.C. Estoque, Y. Murayama, & S.W. Myint. (2017). Science of the Total Environment Effects of landscape composition and Pattern on land surface temperature: An urban heat island study in the Megacities of Southeast Asia. *Science of the Total Environment*, *577*, 349-359.

[7] T.M. Giannaros & D. Melas. (2012). Study of the urban heat island in a coastal Mediterranean City: The case study of Thessaloniki, Greece. *Atmospheric Research*, *118*, 103-120.

[8] S. W.Myint, A. Brazel, G. Okin, & A. Buyantuyev. (2010). Combined effects of impervious surface and vegetation cover on air temperature variations in a rapidly expanding desert city. *GIScience & Remote Sensing*, *47*(3), 301-320.

[9] T.R. Oke. 1997. Urban Climates and Global Environmental Change. In: Thompson, R.D. and A. Perry (eds.) Applied Climatology: Principles & Practices. New York, NY: Routledge. pp. 273-287.

[10] D. Roemmich & J. Gilson. (2009). The 2004–2008 mean and annual cycle of temperature, salinity, and steric height in the global ocean from the Argo Program. *Progress in Oceanography*, *82*(2), 81-100.

[11] P. Shahmohamadi, A. Che-Ani, K.N.A Maulud, A. Sairi & M.F.I. Mohd-Nor. (2010). The framework to mitigate the urban heat island effect for improving the environment and protecting human health. *International Journal of Sustainable Development and Planning*, *5*(4), 351-366.

[12] N. Shamloo, M.Taghi Sattari, H. Apaydin, K. Valizadeh Kamran & R. Prasad. (2021). Evapotranspiration estimation using SEBAL algorithm integrated with remote sensing and experimental methods. *International Journal of Digital Earth*, *14*(11), 1638-1658.

[13] R. Shih and D. Ty. (2013). The Urban Heat Island (UHI) Phenomenon in Cebu City, Philippines: An Initial Study. Retrieved from https://www.researchgate.net/publication/275152563

[14] J.Voogt. (2002). Urban Heat Island. In Munn, T. (ed.) Encyclopedia of Global Environmental Change, Vol. 3. Chichester: John Wiley and Sons.

[15] Q.Weng, D., Lu, & J.Schubring,. (2004). Estimating land surface temperature–vegetation abundance relationship for urban heat island studies. *Remote sensing of Environment*, *89*(4), 467-483.